# Reservoir Computing with Mycelium-Inspired Memristive Oscillating Cellular Automata

Theodoros Panagiotis Chatzinikolaou*, Alexandros Mavropopoulis*, Ioannis Tompris*, Georgios Kleitsiotis*, Ioannis K. Chatzipaschalis*†, Karolos-Alexandros Tsakalos*, Iosif-Angelos Fyrigos*, Michail-Antisthenis Tsompanas‡, Andrew Adamatzky‡, Panagiotis Dimitrakis§, and Georgios Ch. Sirakoulis*

* Department of Electrical and Computer Engineering, Democritus University of Thrace, Xanthi, Greece

† Department of Electronic Engineering, Universitat Politécnica de Catalunya, Barcelona, Spain

‡ Department of Computer Science and Creative Technologies, University of the West of England, Bristol, UK

§ Institute of Nanoscience and Nanotechnology, NCSR Demokritos, Athens, Greece

***Abstract*—This paper presents a mycelium-inspired reservoir network through an innovative extension of the Memristive Oscillating Cellular Automata (MOCA) circuit-based network. Drawing on the adaptive, self-organizing properties of mycelium, this MOCA grid employs $SiN_x$-based RRAMs to form reconfigurable, dynamic connections that replicate mycelial network behaviors. Using the Stanford-PKU RRAM model, the non-linear properties of the fabricated devices have been characterized, establishing a flexible reservoir network, capable of transforming and encoding input signals. MOCA topology showcases its suitability as a low-power, hardware-compatible RC model. The network has been evaluated, demonstrating small-world characteristics, including high clustering and short average path lengths, critical for effective information propagation and complex local dynamics. The resulting adaptable circuit offers a scalable foundation for future applications in bio-inspired reservoir computing.**

***Index Terms*—Engineered Living Materials, Mycelium, Cellular Automata, Memristive Oscillator, Memristive Digital Twin, Reservoir Computing**

## I. Introduction

Mycelium, the vegetative network of fungi, has drawn attention as a promising candidate for bio-inspired computing systems due to its adaptive, self-organizing network structure. Its natural ability to form intricate, hierarchical networks supports robust connectivity, communication, and resilience, which make it an ideal candidate for bio-inspired computing models, especially those aiming to mimic complex, dynamic interactions within a network [1], [2]. Mycelium's complex connectivity, position it as an ideal candidate for implementing reservoir computing (RC) networks, a computational paradigm particularly well-suited for processing temporal data and complex, non-linear dynamics.

Reservoir computing (RC) is designed to exploit the dynamic properties of a network, where a "reservoir" layer, typically a recurrent neural network or a similarly structured dynamic system, encodes and processes temporal data. By providing high-dimensional mappings of input signals, RC enables powerful pattern recognition, classification, and time-series prediction capabilities with relatively simple readout mechanisms [3]–[5]. The potential of RC aligns with mycelium's biological network structure, which can naturally facilitate non-linear and transient signal processing similar to RC frameworks. Mycelium's network, with its evolving connectivity and plasticity, thus serves as a compelling bio-inspired model for RC networks that need to handle adaptive and real-time processing demands [6].

Implementing mycelium-inspired architectures on hardware, however, presents significant challenges [7]. Existing models that capture mycelium's evolution have mainly been limited to software or digital hardware implementations due to the high computational resources required, which constrains practical deployment [8]–[11]. A direct analog hardware implementation that captures the adaptive and network-like qualities of mycelium would enable efficient, real-time reservoir computing applications but requires a solution capable of managing complex, non-linear interactions without high power demands or excessive complexity.

Resistive Random Access Memory (RRAM) technology offers a promising approach for this hardware implementation [12], [13]. RRAMs, as non-volatile, memory-retentive devices, can emulate the adaptable and memory-preserving properties observed in mycelium networks [9]. Their low-power requirements and non-linear response characteristics have made RRAMs ideal for neuromorphic computing, where they replicate key synaptic behaviors [14], supporting the implementation of hardware-efficient, low-power circuits that can retain the non-linear, oscillatory dynamics essential for reservoir computing [15], [16]. When combined with RRAMs, reservoir computing can process non-linear patterns and oscillatory interactions, emulating biological networks [6].

In this work, the prior MOCA circuit-based network [17] is extended, and introduced as a mycelium-structured reservoir computing (RC) framework. Here, the MOCA network utilizes the adaptive and self-organizing growth mechanisms inspired by the mycelium to form an RC network. The integration of SiNx-based RRAMs in the MOCA network allows for reconfigurable connections, accurately reflecting the dynamic connectivity of mycelium networks. The RRAMs were fabricated, tested and programmed, with device characteristics fitted using the Stanford-PKU RRAM model. This design employs the inherent non-linearity of RRAs within the MOCA framework to establish a reservoir capable of high-dimensional representation and transformation of input signals. The design along with its topology evaluation metrics of the Mycelium-

This work has been supported by the framework of the FUNGATERIA project, which has received funding from the European Union's HORIZON-EIC-2021-PATHFINDER CHALLENGES program under grant agreement No. 101071145.

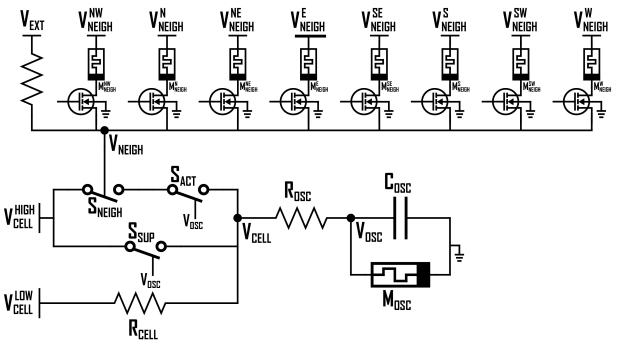


Fig. 1. Memristive Oscillating Cellular Automaton (MOCA) cell circuit with $SiN_x$-based MIS devices.

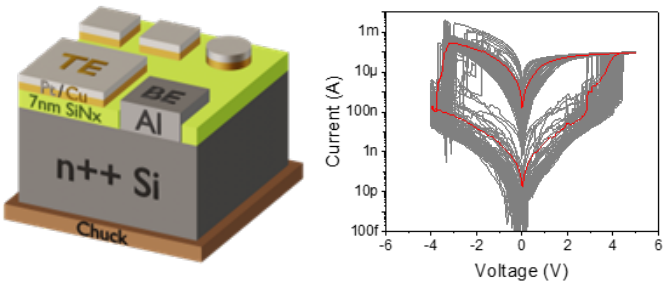


(a) (b)

Fig. 2. (a) Fabricated MIS device's structure, and (b) I-V curves of the first 100 cycles (their average is shown in red).

inspired RC network are demonstrated, proving the MOCA grid's viability as a low-power, hardware-compatible RC network capable of efficient temporal data processing.

## II. Reconfigurable MOCA Cell Through $SiN_x$-based MIS Devices

A reconfigurable MOCA network is being utilized to implement mycelium-based reservoir networks. The MOCA configuration leverages the parallelism of Cellular Automata (CA) [18] and the unique properties of memristive devices to achieve efficient hardware computations [19]. By assembling MOCA cells into a spatial grid, the behavior of ELMs can be emulated, focusing on their growth and evolution processes. The collective output oscillations from all grid cells demonstrate complex dynamics and pattern formation potential, reflecting biological system functionalities and paving the way for bio-inspired computing architectures [17].

### A. The MOCA Cell

Each MOCA cell (Fig. 1) features an output voltage oscillation mechanism that fluctuates within specified voltage thresholds set by a unipolar RRAM device ($M_{OSC}$). The device is configured as a single-layer Metal-Insulator-Metal (MIM) structure composed of Ag ($\sim 40\,\mathrm{nm}$) / $SiO_2$ ($\sim 20\,\mathrm{nm}$) / Pt NPs ($\sim 5\,\mathrm{nm}$), exhibiting rapid switching capabilities crucial for achieving the desired oscillation phenomena [20], and is modeled using a physics-driven approach with a compact set of equations formulated in Verilog-A [21]. Oscillation initiation requires a constant DC voltage, with sustained oscillations ensured by appropriately configuring the $R_{OSC}$ and $C_{OSC}$ values to prevent voltage equilibrium across the RRAM. Incorporating switches and $V_{CELL}^{HIGH;LOW}$ voltage supplies ensures proper MOCA operation, prevents abrupt oscillation interruptions, and allows controlled transitions between its operational phases.

An external voltage supply ($V_{EXT}$), representing stimuli such as humidity, nutrients, or light affecting the hyphae evolution, is applied alongside neighboring voltages. This setup allows for the definition of distinct MOCA rules by influencing the connecting node voltage $V_{NEIGH}$ from neighbors signals. Adjusting $V_{EXT}$ modulates the threshold of the $S_{NEIGH}$, enabling varied behaviors for each cell and emulating complex biological processes. The MOCA cell operates in three distinct phases, namely resting, activation, and suppression. During the resting phase, the oscillating unit remains idle. Activation occurs when a stimulus exceeds the MOCA activation threshold, triggering oscillatory behavior analogous to the activator of reaction-diffusion systems. The suppression phase follows, where the oscillation diminishes before returning to the resting state, mirroring the suppressor behavior in such systems.

### B. $SiN_x$-based MIS Devices

To further enhance the fitting capabilities of the MOCA configuration, the neighboring input signals are reaching their joint node through our fabricated memristive $SiN_x$-based MIS devices arranged in a 1T1R configuration to allow both functioning and programming operations, as it can be observed in Fig. 1. This introduces grid reconfigurability, allowing the network to dynamically emulate various mycelium patterns and morphologies. The properties of the utilized bipolar RRAMs enable them to act as adjustable reconfigurable connections between MOCA cells, which is crucial for implementing a reservoir computing system, where the rich dynamics and state-dependent responses of the memristive network serve as a computational reservoir. By leveraging these properties, the system can perform complex temporal processing tasks, mimicking the information processing capabilities observed in biological networks.

The $SiN_x$-based RRAMs were simulated with the Stanford-PKU RRAM model, a SPICE-compatible compact model, fitted to the I-V characteristics of the fabricated devices (Fig. 2(b)). This model can properly describe the switching behavior of bipolar metal oxide RRAM, taking into account factors such as the electric field, temperature-enhanced oxygen ion migration, and local temperature due to Joule heating [22].

The MIS devices were fabricated using N-type silicon wafers, which underwent cleaning with Piranha and $10\%$ HF solutions, followed by the growth of a $10nm$ thick sacrificial oxide layer through dry oxidation. Phosphorus ion implantation ($40keV, 10^{15}cm^{-2}$) has been performed, and a rapid thermal annealing at $1050°C$ for $20s$ followed. After removing the oxide layer and re-cleaning, a $7nm$ $SiN_x$ ($x = 1.27$) was deposited by LPCVD at $810°C$. Electron beam lithography

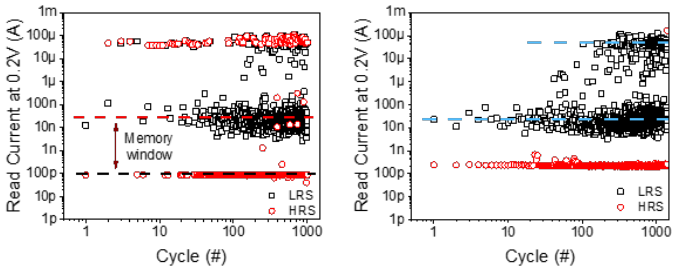


Fig. 3. Read current at 0.2 V after each SET/RESET cycle (a) without changing the SET/RESET conditions at each cycle, and (b) with dynamically adjustment of the conditions.

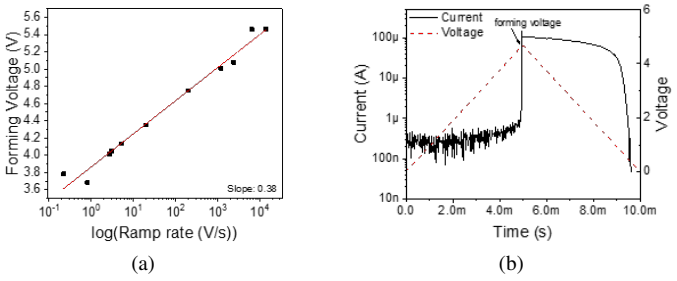


Fig. 4. (a) Forming voltage versus the logarithm of ramp rate, and (b) typical VR and resulted current waveform.

has been employed to form the bottom electrode (BE) and top electrode (TE); $100nm$ were deposited for the BE via thermal evaporation, while the TE consisted of $30nm$ of copper and $30nm$ of platinum deposited by sputtering (Fig. 2(a)). The device has an area of $50 \times 50\mu m^2$ with both electrodes located on the front side of the wafer. Electrical measurements of the I-V characteristics were conducted at room temperature in ambient air ($RH = 45\%$) using HP4155A and Tektronix 4200A analyzers, along with an Agilent 33120A function generator. A Cascade Summit 12000 prober facilitated device contact, applying voltage to the TE while grounding the BE.

## III. Mycelium Morphological Evolution and RRAM Programming for Reservoir Computing

To align the MOCA network with mycelium-like structures, a weight extraction algorithm is employed based on [9] to transfer the CA model's growth pattern dynamics as RRAM weights. This process enables the MOCA network to mimic the connectivity and network characteristics of the biological mycelium model. By extracting and mapping these weights directly, the MOCA network can replicate mycelium network structures, ensuring that the dynamics within the mycelium-based reservoir have been transferred into the designed circuit. The 1T1R topology is utilized on its programming operation, isolating the device to apply the necessary voltage to properly program the $SiN_x$-based MIS RRAM devices to the algorithm's weights. For achieving the necessary memristive state, the voltage ramp (VR) programming method is employed over the conventional voltage sweep (VS) approach. Voltage ramps are particularly advantageous due to their lower power consumption and more easy to control the filament's

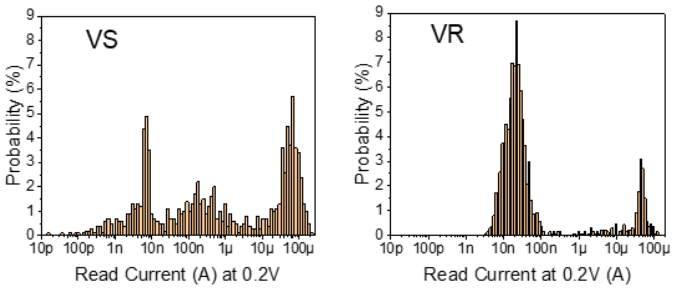


Fig. 5. Distribution of LRS read current at $0.2V$ for samples operated using (a) VS, and (b) VR.

formation [23]. The devices were programmed using a ramp up to $4.7V$ for SET with a rise time of $5ms$, corresponding to a ramp rate of $940V/s$, and a ramp down to $-5V$ for RESET with a rise time of $2.5ms$, equating to 2000 V/s. These parameters were chosen after statistically analyzing a variety of ramp rates and voltages.

The state of the device is read, after each successful programming at the low/high resistance state (LRS/HRS) at a voltage of $0.2V$, leading to the results shown in Fig. 3a, which $848$ successful cycles were achieved. However, it is observed that a lot of times the RESET was not successful, and the device didn't revert back to a HRS. To further improve the endurance, the Tektronix 4200A parameter analyzer was controlled by a Python script, in order to dynamically increase at a first manner the rise time and then the voltage of the ramps, as needed by the measuring device to successfully transition from HRS to LRS and vice versa. In this way, the endurance of RRAM devices has been significantly improved, allowing for over $1400$ cycles without substantial degradation, as shown in Fig. 3b. The forming voltage is analogous to the logarithmic of the ramp rate as Fig. 4a showcases. In accordance to that, the consuming power increases as well along with the ramp rate, so the latter has been properly chosen to minimize the thermal stress and extend device's lifespan. The power increase is indicated by the logarithmic rise of current with respect to voltage, shown in Fig. 4b, producing a very small power integral and therefore lowering consumption.

A comparison of voltage ramps and sweeps was performed for over $100$ cycles, to showcase the robustness of the preferred programming scheme. It was found that the formation of thinner conductive filaments, which are easier to dissolve during RESET, ensures more reliable data retention and enhances the stability of the LRS. As a result, the distribution of LRS current using the voltage sweep scheme, depicted in Fig. 5a is not as discernible as the distribution using the voltage ramps, where two distinct states are observed, as shown in Fig. 5b. Thus, VR is a better way to achieve the highest endurance for $SiN_x$-based MIS RRAMs than VS. This is because VR leads to the formation of thinner filaments that can be dissolved easier during the RESET, thus delaying the permanent breakdown of the device when compared to the VS.

## IV. Reservoir Evaluation Metrics

To evaluate the MOCA network's potential for reservoir computing, we focus on three key metrics derived from the adjacency matrix $A$, where each entry $A_{ij}$ represents the presence of a connection from node $i$ to node $j$. These metrics are selected to highlight the small-world characteristics—such as short path lengths and high clustering—required for effective information processing in reservoir computing systems [24]. Average Path Length ($APL$) is essential for assessing how efficiently information propagates across the network. Defined as the mean shortest path between all pairs of nodes, APL is calculated by:

$$APL = \frac{1}{N(N-1)} \sum_{i \neq j} d(i,j) \tag{1}$$

where $d(i,j)$ is the shortest path distance between nodes $i$ and $j$, and $N$ is the total number of nodes. A low APL indicates that information can travel quickly through the network, a key property for the responsive dynamics necessary in reservoir computing [4]. The Clustering Coefficient ($C_i$) measures the tendency of nodes to form tightly connected groups, which supports localized, complex dynamics within the network. For each node $i$, the clustering coefficient $C_i$ is given by:

$$C_i = \frac{\sum_{j,k} A_{ij} A_{jk} A_{ki}}{\deg(i)(\deg(i)-1)} \tag{2}$$

where $\deg(i)$ is the degree of node $i$. High clustering is characteristic of small-world networks and enhances the network's ability to produce varied, context-sensitive responses essential for reservoir computing applications [25].

These metrics provide a comprehensive evaluation of the MOCA network's small-world characteristics and its suitability as a reservoir, supporting dynamic information processing capabilities essential for reservoir computing.

TABLE I
Evaluation Metrics for 30 Different Samples of Mycelium-based RC Designs

| Sample - Average Path Length | | Sample - Clustering Coefficient | |
|---|---|---|---|
| 1-1.0758 | 16-1.1818 | 1-0.8053 | 16-0.7612 |
| 2-1.1364 | 17-1.0758 | 2-0.7632 | 17-0.7958 |
| 3-1.0909 | 18-1.1667 | 3-0.8056 | 18-0.7667 |
| 4-1.1364 | 19-1.1818 | 4-0.7723 | 19-0.7304 |
| 5-1.2727 | 20-1.1667 | 5-0.7641 | 20-0.7121 |
| 6-1.1667 | 21-1.2121 | 6-0.7316 | 21-0.7776 |
| 7-1.2424 | 22-1.2121 | 7-0.7359 | 22-0.7507 |
| 8-1.1667 | 23-1.1212 | 8-0.7302 | 23-0.7826 |
| 9-1.2121 | 24-1.0909 | 9-0.7495 | 24-0.7764 |
| 10-1.2576 | 25-1.1818 | 10-0.7128 | 25-0.7718 |
| 11-1.2727 | 26-1.1667 | 11-0.7398 | 26-0.7690 |
| 12-1.0758 | 27-1.2121 | 12-0.8052 | 27-0.7440 |
| 13-1.2727 | 28-1.1212 | 13-0.6984 | 28-0.7507 |
| 14-1.1212 | 29-1.2273 | 14-0.7654 | 29-0.7076 |
| 15-1.2424 | 30-1.1818 | 15-0.7261 | 30-0.7834 |
| **Avg - 1.1747** | | **Avg - 0.7562** | |

## V. Evaluation Results

The mycelium-inspired MOCA network is evaluated as a reservoir computing framework using two key metrics that define small-world networks: Average Path Length ($APL$), and Clustering Coefficient ($C_i$), and Spectral Radius. These metrics underscore the MOCA network's balance between efficient information flow, complex local dynamics, and stability. Fig. 6 compares $APL$ and $C_i$, showcasing the network's small-world traits advantageous for reservoir computing. The low APL and high clustering coefficient signify the network's ability to propagate information efficiently while maintaining adaptability.

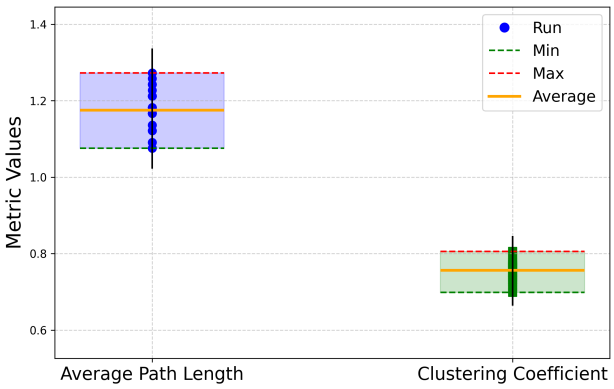


Fig. 6. Comparison of Average Path Length and Clustering Coefficient in Mycelium-Based Network.

Specifically, $APL$ values average 1.175 across configurations, with a range from 1.075 to 1.273, indicating fast information transfer across nodes. These values align with typical small-world expectations, presenting both fast data flow and structural adaptability. Similarly, $C_i$ values average 0.756, spanning 0.698 to 0.805. This high clustering indicates a strong tendency for nodes to form dense clusters, supporting localized dynamics that produce varied and complex responses. Together, these metrics confirm that the MOCA network's structure mirrors small-world properties, positioning it well for applications requiring dynamic, nonlinear responses. Overall, our results reveal that the MOCA network possesses small-world characteristics conducive to effective reservoir computing. With low APL for fast signal propagation, high clustering for complex localized dynamics, and a substantial spectral radius for stability, the mycelium-inspired MOCA network exhibits the necessary structural properties to serve as a powerful and efficient reservoir computing model.

## VI. Conclusions

In conclusion, this work presents a method to utilize mycelium networks as reservoir computing systems and implement them at circuit level through a reconfigurable MOCA network with $SiN_x$-based RRAMs. The mycelium's growth and connectivity are translated into RRA weight configurations. These weights are then programmed into the MOCA network, enabling the RRAMs to represent the mycelium's connectivity. The resulting circuit achieves efficient hardware implementation of mycelium-inspired reservoir networks, providing an adaptable and scalable approach for future reservoir computing applications.

## REFERENCES


[1] A. Adamatzky, P. Ayres, A. E. Beasley, N. Roberts, and H. A. Wösten, "Logics in fungal mycelium networks," *Logica Universalis*, vol. 16, no. 4, pp. 655–669, 2022.

[2] M. R. Islam, G. Tudryn, R. Bucinell, L. Schadler, and R. Picu, "Morphology and mechanics of fungal mycelium," *Scientific reports*, vol. 7, no. 1, p. 13070, 2017.

[3] K.-A. Tsakalos, G. C. Sirakoulis, A. Adamatzky, and J. Smith, "Protein structured reservoir computing for spike-based pattern recognition," *IEEE Transactions on Parallel and Distributed Systems*, vol. 33, no. 2, pp. 322–331, 2021.

[4] K. Nakajima and I. Fischer, *Reservoir computing*. Springer, 2021.

[5] A. Passias, K.-A. Tsakalos, I. Kansizoglou, A. M. Kanavaki, A. Gkrekidis, D. Menychtas, N. Aggelousis, M. Michalopoulou, A. Gasteratos, and G. C. Sirakoulis, "A biologically inspired movement recognition system with spiking neural networks for ambient assisted living applications," *Biomimetics*, vol. 9, no. 5, p. 296, 2024.

[6] C. Du, F. Cai, M. A. Zidan, W. Ma, S. H. Lee, and W. D. Lu, "Reservoir computing using dynamic memristors for temporal information processing," *Nature communications*, vol. 8, no. 1, p. 2204, 2017.

[7] A. Adamatzky, P. Ayres, G. Belotti, and H. Wösten, "Fungal architecture position paper." *International Journal of Unconventional Computing*, vol. 14, 2019.

[8] V. Carlström, A. Rigobello, and P. Ayres, "Modelling of morphogenesis to support the design of fungal-based engineered living materials," *Research Directions: Biotechnology Design*, vol. 2, p. e11, 2024.

[9] I. Tompris, I. K. Chatzipaschalis, T. P. Chatzinikolaou, I.-A. Fyrigos, M.-A. Tsompanas, A. Adamatzky, P. Ayres, and G. C. Sirakoulis, "A reaction-diffusion cellular automata model for mycelium-based engineered living materials evolution," in *International Conference on Cellular Automata for Research and Industry*. Springer, 2024, pp. 253–264.

[10] M. D. Fricker, L. L. Heaton, N. S. Jones, and L. Boddy, "The mycelium as a network," *The fungal kingdom*, pp. 335–367, 2017.

[11] I. K. Chatzipaschalis, I. Tompris, K. Rallis, T. P. Chatzinikolaou, I.-A. Fyrigos, M.-A. Tsompanas, A. Adamatzky, P. Ayres, A. Rubio, and G. C. Sirakoulis, "Mycelium-based elm digital twin implemented in fpga," in *International Conference on Cellular Automata for Research and Industry*. Springer, 2024, pp. 265–276.

[12] E. Tsipas, T. P. Chatzinikolaou, K.-A. Tsakalos, K. Rallis, R.-E. Karamani, I.-A. Fyrigos, S. Kitsios, P. Bousoulas, D. Tsoukalas, and G. C. Sirakoulis, "Unconventional memristive nanodevices," *IEEE Nanotechnology Magazine*, vol. 16, no. 6, pp. 34–45, 2022.

[13] ——, "Unconventional computing with memristive nanocircuits," *IEEE Nanotechnology Magazine*, vol. 16, no. 6, pp. 22–33, 2022.

[14] A. Mehonic, A. Sebastian, B. Rajendran, O. Simeone, E. Vasilaki, and A. J. Kenyon, "Memristors—from in-memory computing, deep learning acceleration, and spiking neural networks to the future of neuromorphic and bio-inspired computing," *Advanced Intelligent Systems*, vol. 2, no. 11, p. 2000085, 2020.

[15] M. S. Kulkarni and C. Teuscher, "Memristor-based reservoir computing," in *Proceedings of the 2012 IEEE/ACM International Symposium on Nanoscale Architectures*, 2012, pp. 226–232.

[16] R. Midya, Z. Wang, S. Asapu, X. Zhang, M. Rao, W. Song, Y. Zhuo, N. Upadhyay, Q. Xia, and J. J. Yang, "Reservoir computing using diffusive memristors," *Advanced Intelligent Systems*, vol. 1, no. 7, p. 1900084, 2019.

[17] T. P. Chatzinikolaou, I. Tompris, I. K. Chatzipaschalis, I.-A. Fyrigos, M.-A. Tsompanas, A. Adamatzky, and G. C. Sirakoulis, "Mycelium-based elm emulation utilizing memristive oscillating cellular automata," in *2024 IEEE 24th International Conference on Nanotechnology (NANO)*. IEEE, 2024, pp. 551–556.

[18] G. C. Sirakoulis, *Cellular Automata Hardware Implementation*. Berlin, Heidelberg: Springer Berlin Heidelberg, 2018, pp. 1–29.

[19] T. P. Chatzinikolaou, I.-A. Fyrigos, V. Ntinas, S. Kitsios, P. Bousoulas, M.-A. Tsompanas, D. Tsoukalas, A. Adamatzky, and G. C. Sirakoulis, "Wave cellular automata for computing applications," in *2022 IEEE International Symposium on Circuits and Systems (ISCAS)*, 2022, pp. 3463–3467.

[20] P. Bousoulas, S. Kitsios, T. P. Chatzinikolaou, I.-A. Fyrigos, V. Ntinas, M.-A. Tsompanas, G. C. Sirakoulis, and D. Tsoukalas, "Material design strategies for emulating neuromorphic functionalities with resistive switching memories," *Japanese Journal of Applied Physics*, vol. 61, no. SM, p. SM0806, 2022.

[21] I.-A. Fyrigos, T. P. Chatzinikolaou, V. Ntinas, S. Kitsios, P. Bousoulas, M.-A. Tsompanas, D. Tsoukalas, A. Adamatzky, A. Rubio, and G. C. Sirakoulis, "Compact thermo-diffusion based physical memristor model," in *2022 IEEE International Symposium on Circuits and Systems (ISCAS)*. IEEE, 2022, pp. 2237–2241.

[22] H. Li, Z. Jiang, P. Huang, Y. Wu, H.-Y. Chen, B. Gao, X. Y. Liu, J. F. Kang, and H.-S. P. Wong, "Variation-aware, reliability-emphasized design and optimization of rram using spice model," in *2015 Design, Automation & Test in Europe Conference & Exhibition (DATE)*, 2015, pp. 1425–1430.

[23] G. Sassine, C. Cagli, J.-F. Nodin, G. Molas, and E. Nowak, "Novel computing method for short programming time and low energy consumption in hfo 2 based rram arrays," *IEEE Journal of the Electron Devices Society*, vol. 6, pp. 696–702, 2018.

[24] D. S. Bassett and E. T. Bullmore, "Small-world brain networks revisited," *The Neuroscientist*, vol. 23, no. 5, pp. 499–516, 2017.

[25] C. Gallicchio, A. Micheli, and L. Pedrelli, "Deep echo state networks for diagnosis of parkinson's disease," *arXiv preprint arXiv:1802.06708*, 2018.